

Cell Reports, Volume 43

## Supplemental information

**The ribosomal protein L22 binds the *MDM4*  
pre-mRNA and promotes exon skipping  
to activate p53 upon nucleolar stress**

**Jennifer Jansen, Katherine E. Bohnsack, Susanne Böhlken-Fascher, Markus T. Bohnsack, and Matthias Dobbelstein**

## Supplementary figures and legends

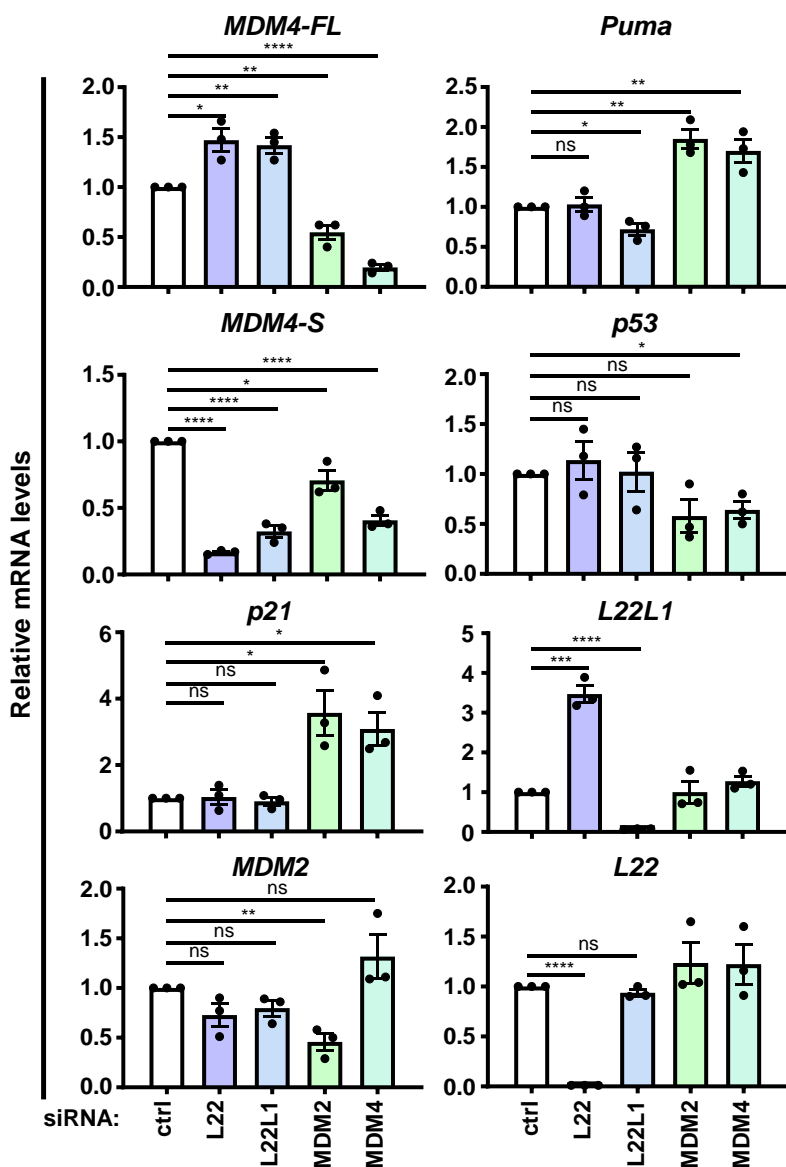
### Figure S1: Gene expression upon L22, L22L1, MDM2 and MDM4 depletion, and nucleoplasmic accumulation of L22 upon 5-FU or BMH-21 treatment.

**A.** RPE cells were transfected with siRNAs to deplete L22, L22L1, MDM2, or MDM4, or with control (ctrl) siRNA, for 48 h. RT-qPCR analyses to detect the indicated target mRNAs were performed, with normalization to the *36B4* (housekeeping gene) mRNA level and then to the control sample. The average of three biological replicates is depicted. Error bars, standard error of the mean. The statistical significance was assessed by an unpaired Student's t test: ns, not significant; \*,  $P \leq 0.05$ ; \*\*,  $P \leq 0.01$ ; \*\*\*,  $P \leq 0.001$ ; \*\*\*\*,  $P \leq 0.0001$ . **B.-G.** RPE cells were treated with 10 or 20  $\mu\text{M}$  5-fluorouracil (5-FU) or 1  $\mu\text{M}$  BMH-21 for 24 h or 48 h to induce nucleolar stress, or they were control-treated (ctrl). **B.-F.** Corresponding to [Figure 1C-E](#). Immunofluorescence was performed to detect L22. **B.-C.** Representative ( $n = 3$ ) images (100x objective, bar: 40  $\mu\text{m}$ ) of the nuclear (DAPI, blue) and L22 (green) staining upon 24 h (**B**) and 48 h treatment (**C**). **D.-E.** Quantification of nuclear intensities of L22 signal in single cells upon 24 h (**D**) and 48 h (**E**) treatment. Red lines represent the mean fluorescence intensity values. A minimum of 180 cells were quantified for each condition. The statistical significance was assessed by a Mann-Whitney U test. The results shown are representative for three biological replicates. **F.** Quantification of cytoplasmic versus nucleoplasmic intensity of the L22 signal. At least 150 cells were analyzed in each case. The average of three biological replicates is depicted. The statistical significance for the fractions "cytoplasmic > nucleoplasmic" and "cytoplasmic = nucleoplasmic" was assessed by an unpaired t test. **G.** Western blot analysis monitoring the levels of the indicated proteins upon induction of nucleolar stress by treatment with 10 or 20  $\mu\text{M}$  5-FU or 1  $\mu\text{M}$  BMH-21 for 24 h. \*, background band. Shown is a representative example of two biological replicates.

# Figure S1

## A

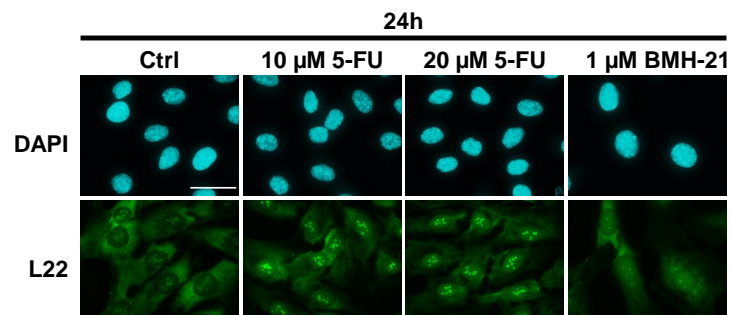
RPE 48h siRNA: L22, L22L1, MDM2, MDM4



## B

RPE

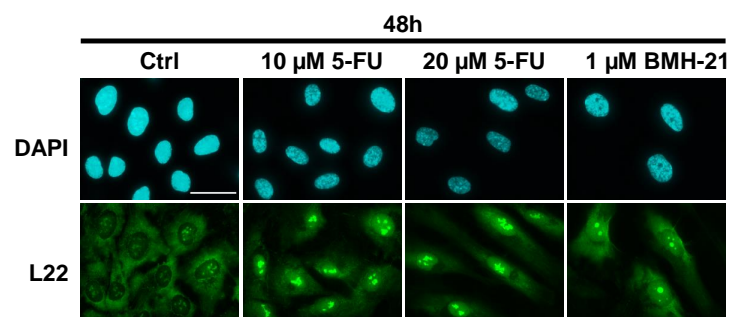
24h 5-FU or BMH-21



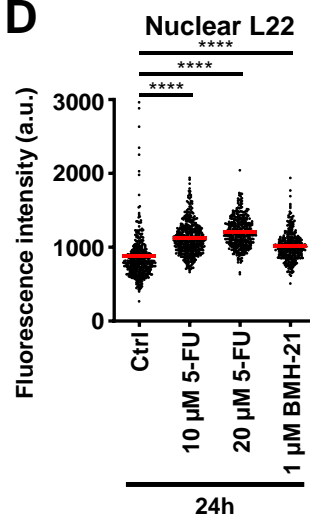
## C

RPE

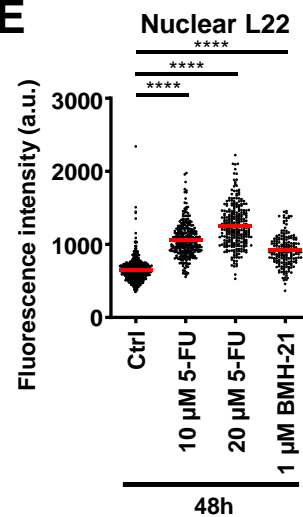
48h 5-FU or BMH-21



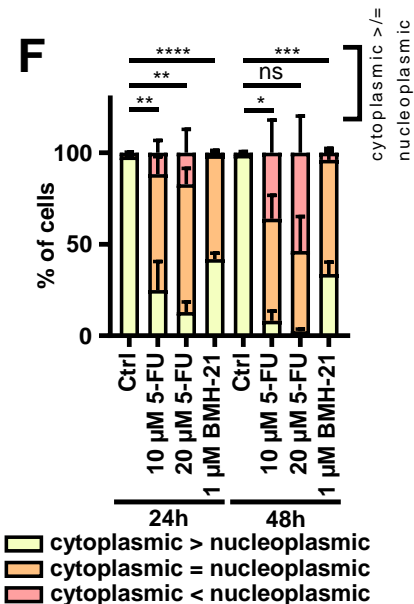
## D



## E



## F



## G

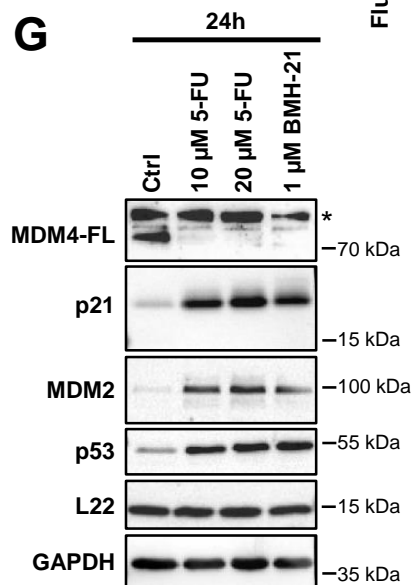
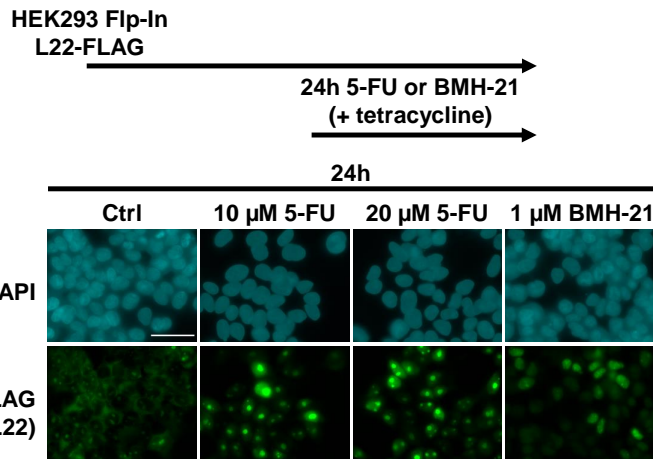


**Figure S2: L22-FLAG accumulation in the nucleoplasm upon treatment with BMH-21 or 5-FU, and *MDM4* exon 6 inclusion upon depletion or overexpression of L22 or L22L1.**

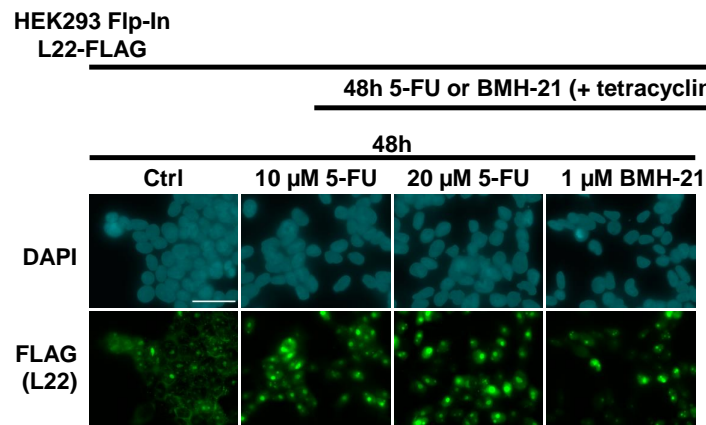
**A.-C.** Stably transfected HEK293 Flp-In cells for the inducible expression of L22-FLAG were treated with 10 or 20  $\mu$ M 5-FU or 1  $\mu$ M BMH-21 for 24 h or 48 h, to induce nucleolar stress. Tetracycline (1  $\mu$ g/mL) was added for all conditions, including the control, during the entire treatment duration (24 h or 48 h), to induce the expression of FLAG-tagged L22. Immunofluorescence staining of L22 using a FLAG antibody was performed. **A.-B.** Representative images (100x objective, bar: 40  $\mu$ m) of the nuclear (DAPI, blue) and L22 (green) staining upon 24 h (**A**) and 48 h treatment (**B**). **C.** Quantification of cytoplasmic versus nucleoplasmic intensity of the L22 signal. At least 100 cells were analyzed in each case. **D.-E.** HEK293T cells were transfected with siRNA to deplete L22 or L22L1 for 48 h. **F.-G.** HEK293T cells were transfected with plasmids to overexpress L22 or L22L1 for 48 h. **D., F.** RT-qPCR analyses to detect the indicated target mRNAs were performed, with normalization to *36B4*. Statistical significance (n = 3): ns, not significant; \*,  $P \leq 0.05$ ; \*\*,  $P \leq 0.01$ ; \*\*\*,  $P \leq 0.001$ ; \*\*\*\*,  $P \leq 0.0001$ . **E., G.** Western blot analyses of the indicated proteins were performed, using GAPDH (**E**) and  $\beta$ -actin (**G**) as sample controls (n = 2).

# Figure S2

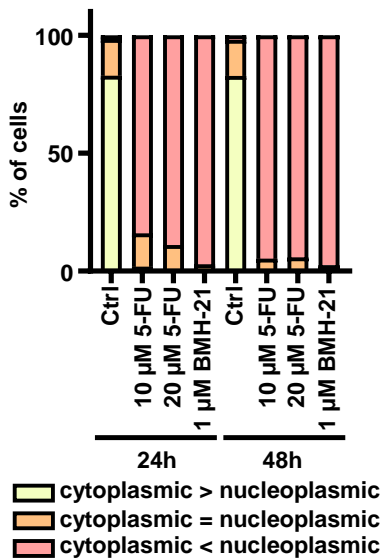
## A



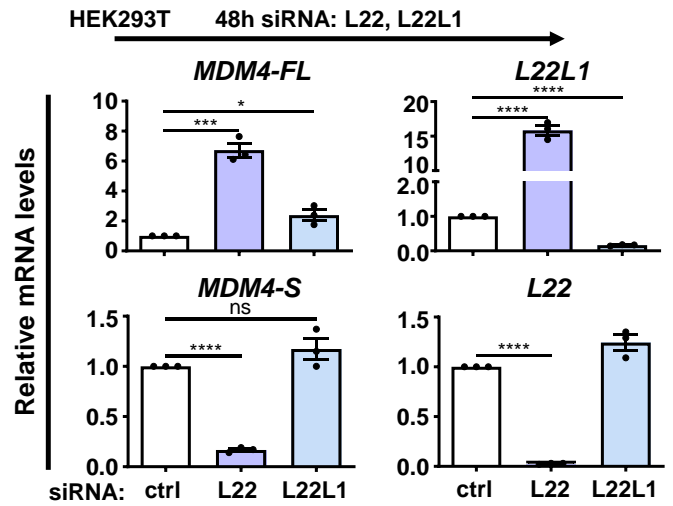
## B



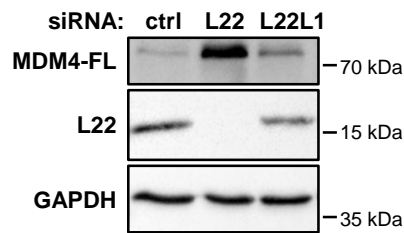
## C



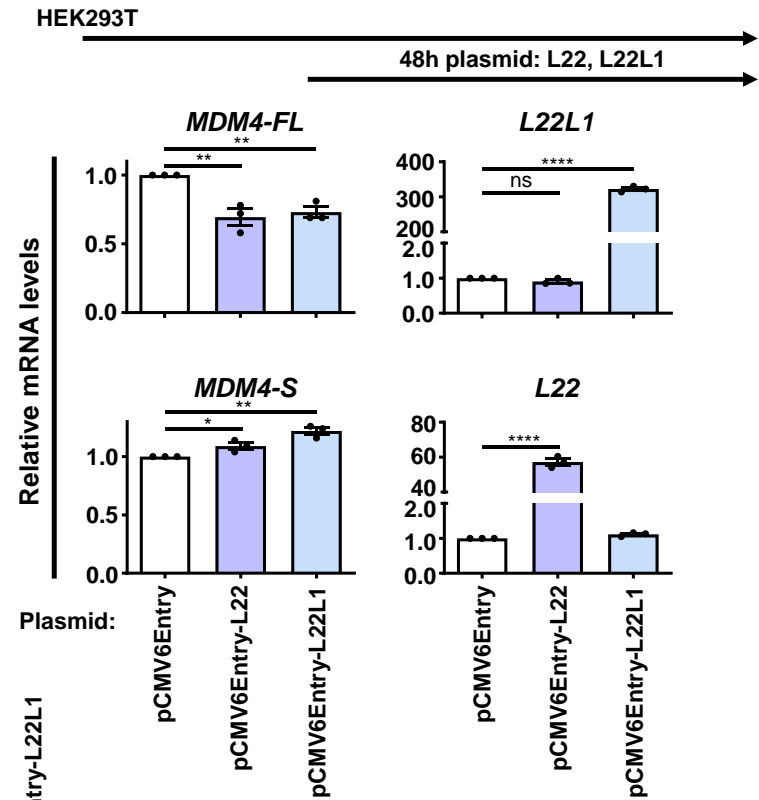
## D



## E



## F



## G

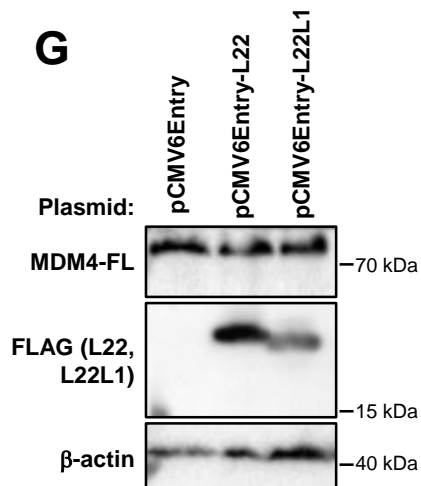


### Figure S3: L22-independent *MDM4* exon skipping.

Corresponding to [Figure 1A-E](#). **A.** Schematic view of exons 3 to 10 of the *MDM4* gene. Yellow boxes represent exons corresponding to their lengths. Primer binding sites in exons 3 and 10, and the lengths of exons 4 to 9 are indicated. **B.** RPE cells were transfected with siRNA to deplete L22 for 48 h, and treated with 1  $\mu$ M BMH-21 for 4 h or 8 h to induce nucleolar stress. RT-qPCR analyses using primers binding in *MDM4* exons 3 and 10, as shown in **A**, were performed with a long (2 min) PCR extension step. PCR products corresponding to the differentially spliced transcripts were visualized using a 5300 Fragment Analyzer (Agilent). Bands of the expected sizes for *MDM4-FL* and *MDM4-S* (skipping exon 6) are marked in orange and red, respectively. The exons from 3 to 10 contained in the respective transcripts, primer binding sites and resulting expected RT-qPCR product lengths are indicated at the bottom. Additionally, bands presumably reflecting the skipping of exon 8 (green) or exons 8 and 9 (blue) are indicated for both *MDM4-FL* (light colours) and *MDM4-S* (dark colours). The results shown are representative for three biological replicates. **C.** Model of L22-dependent and L22-independent *MDM4* exon skipping. L22 promotes *MDM4* exon 6 skipping (red), and L22-independent mechanisms lead to the skipping of exon 8 (green) or exons 8 and 9 (blue).

# Figure S3

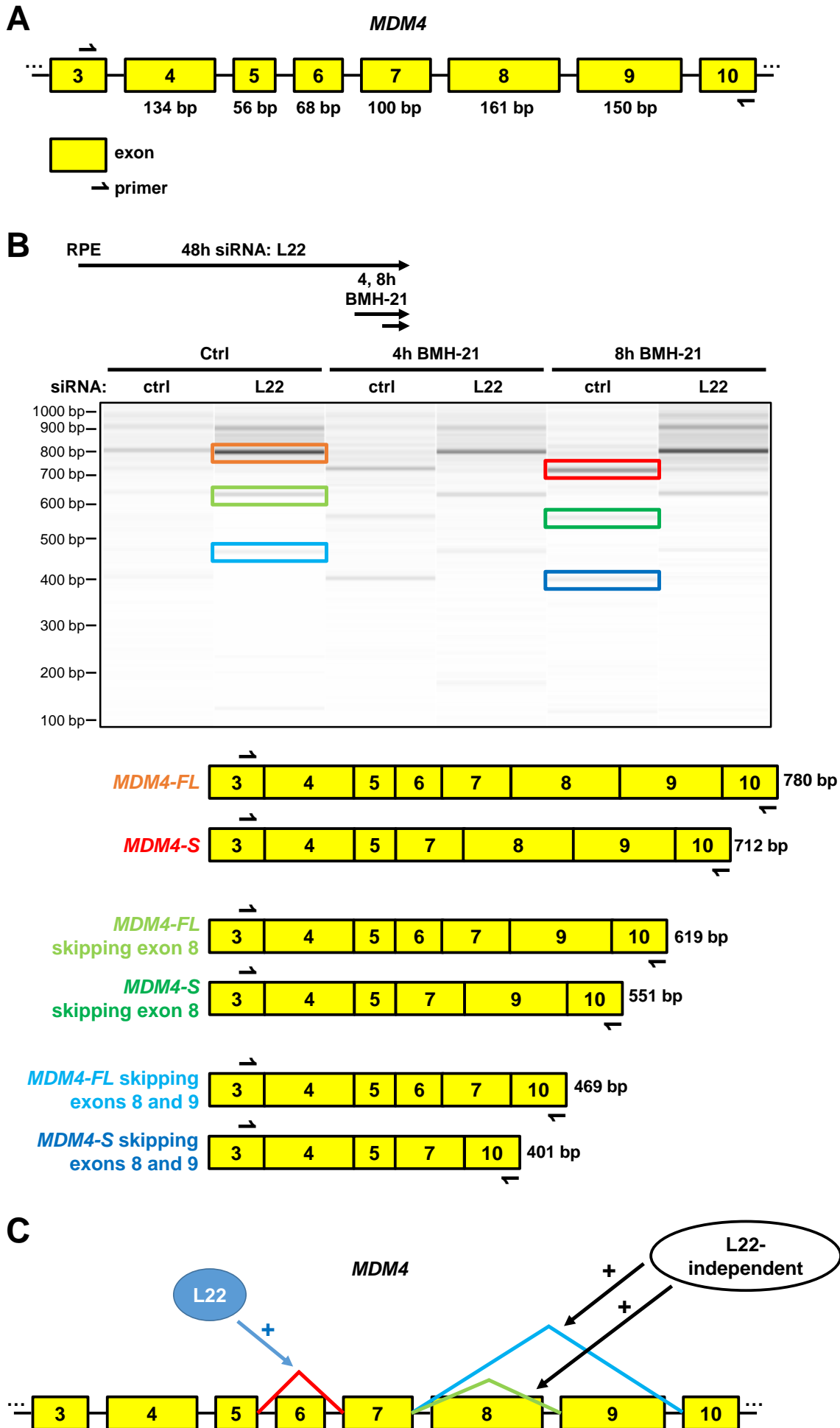
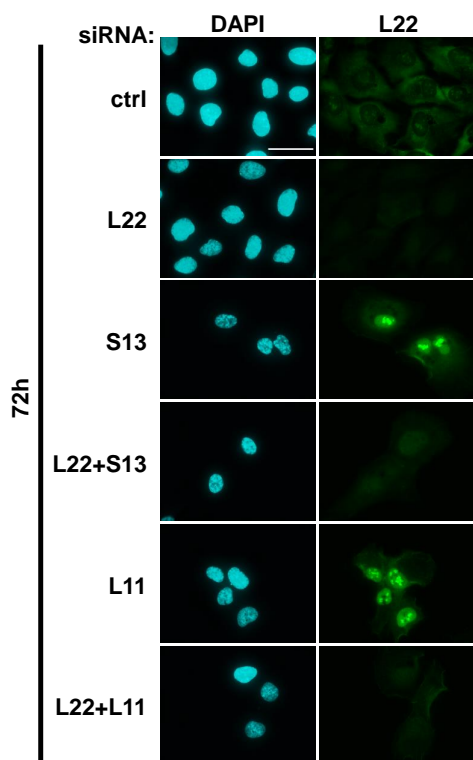


## Figure S4: p53 activity as a function of L22 upon nucleolar stress.

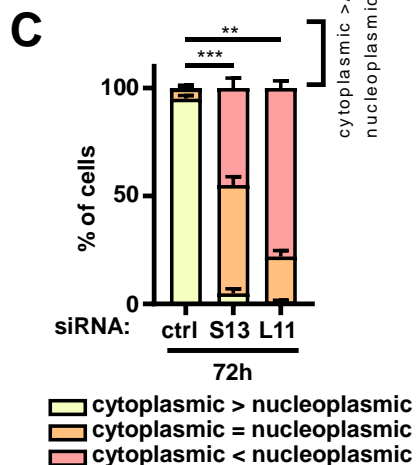
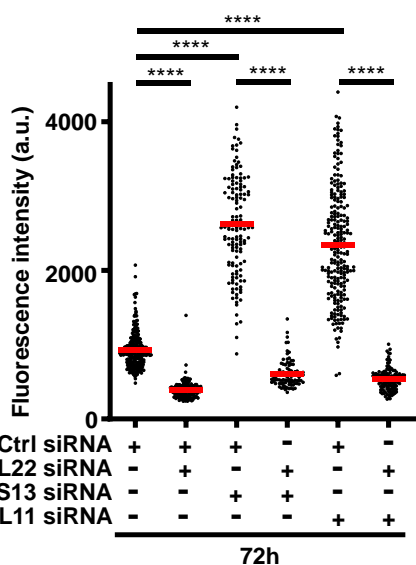
**A.-C.** Corresponding to [Figure 1H-J](#). RPE cells were transfected with siRNA to deplete L22 and/or S13 or L11 for 72 h. Immunofluorescence staining of L22 was performed (n = 3). **A.** Images (100x objective, bar: 40  $\mu$ m) of the nuclear (DAPI, blue) and L22 (green) staining. **B.** Quantification of single nuclear intensities of the L22 signal. Red lines represent the mean fluorescence intensity values. A minimum of 90 cells were quantified for each condition. The statistical significance was assessed by a Mann-Whitney U test: ns, not significant; \*,  $P \leq 0.05$ ; \*\*,  $P \leq 0.01$ ; \*\*\*,  $P \leq 0.001$ ; \*\*\*\*,  $P \leq 0.0001$ . **C.** Quantification of cytoplasmic versus nucleoplasmic intensity of L22 signal. At least 100 cells were analyzed for each condition. The statistical significance was assessed for all three fractions. **D.-E.** RPE cells were transfected with siRNA to deplete L22 and/or L5 or L11 for 48 h (the latter two to induce nucleolar stress). **D.** RT-qPCR analyses with normalization to *36B4* (n = 3). **E.** Western blot analyses (n = 2). Note that the depletion of L5 also diminishes the levels of L11 and vice versa, presumably due to mutual stabilization of the two proteins within the 5S RNP.

# Figure S4

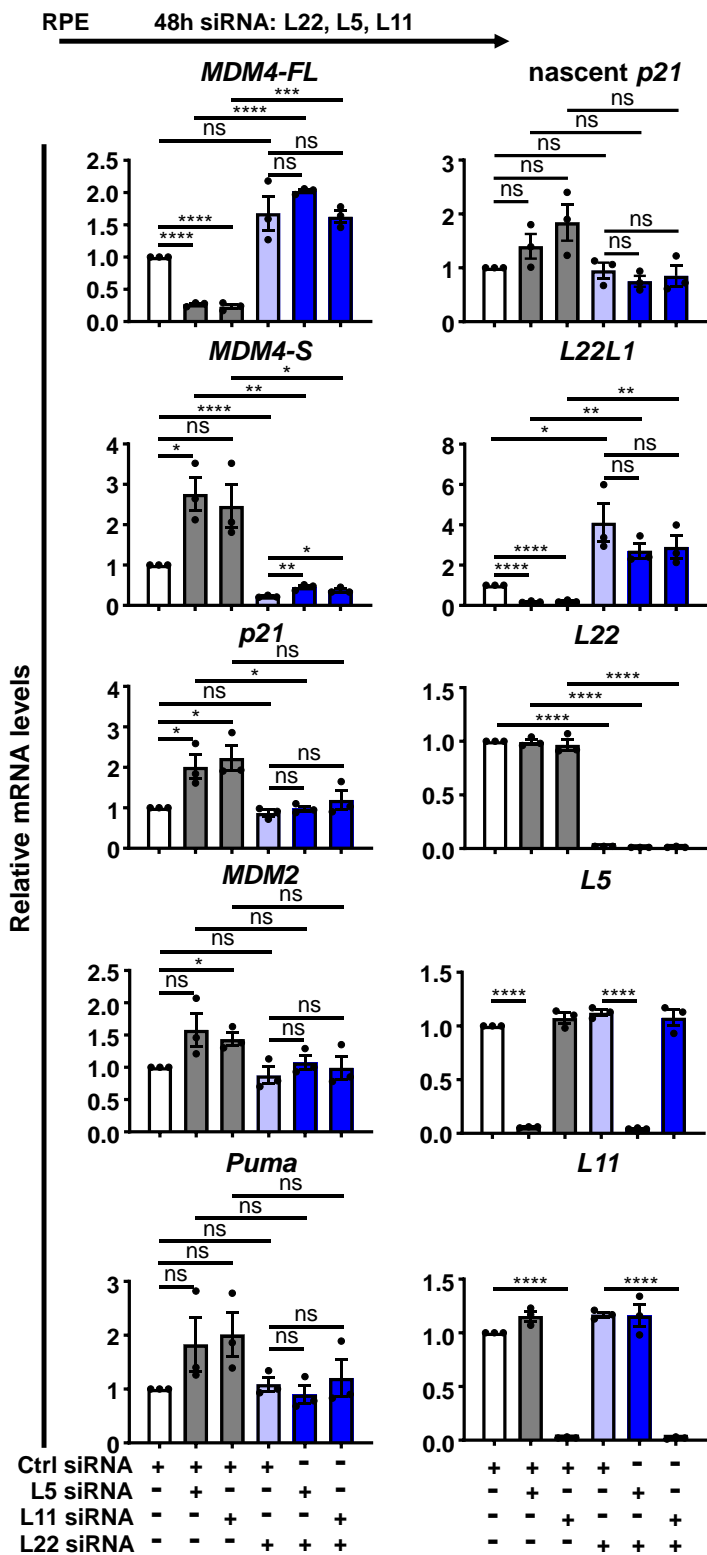
**A** RPE 72h siRNA: L22, S13, L11



**B** Nuclear L22



**D**



**E**

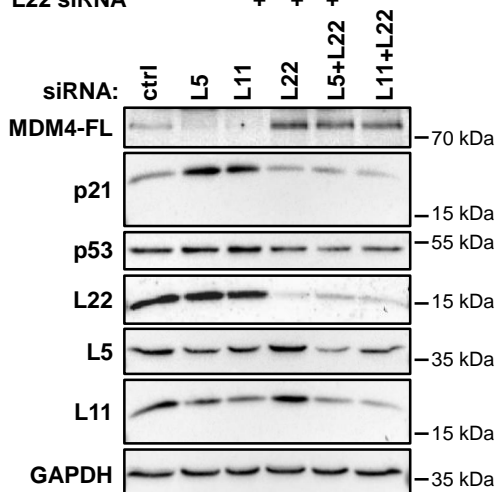


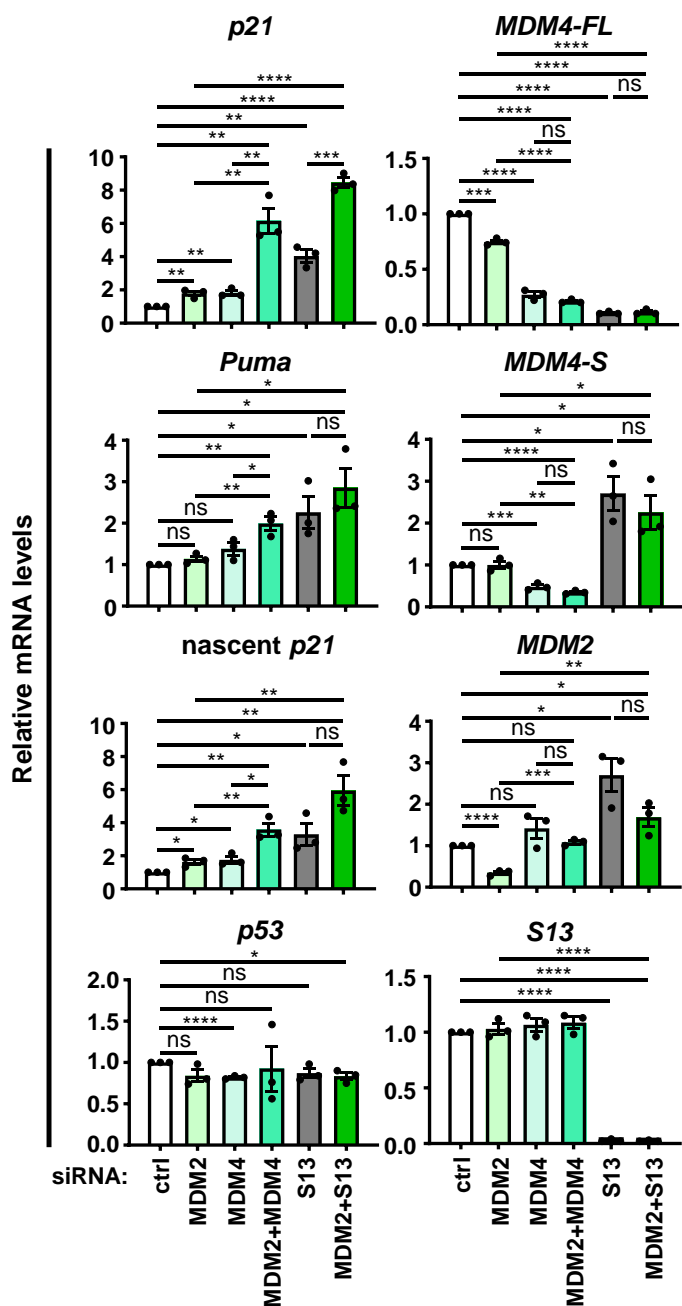
**Figure S5: p53 activity induced by nucleolar stress and MDM4 depletion, and L22-relocalization upon depletion of S13 or L11.**

**A.-B.** RPE cells were transfected with siRNA to deplete MDM2, MDM4, or S13 for 48 h. **A.** RT-qPCR analyses to detect the indicated target mRNAs were performed, with normalization to *36B4*. Statistical significance (n = 3): ns, not significant; \*,  $P \leq 0.05$ ; \*\*,  $P \leq 0.01$ ; \*\*\*,  $P \leq 0.001$ ; \*\*\*\*,  $P \leq 0.0001$ . **B.** Western blot analysis (n = 2). \*, background bands. Triangle symbol indicates band of interest. **C.-E.** Stably transfected HEK293 Flp-In cells for the inducible expression of L22-FLAG were transfected with siRNA to deplete L22. To cause nucleolar stress, S13 or L11 were depleted in parallel, for 48 h or 72 h. 24 h after seeding and reverse siRNA transfection, i.e. for a total duration of 24 h respectively 48 h, tetracycline (1  $\mu\text{g/mL}$ ) was added for all conditions including the control, to induce the expression of FLAG-tagged L22. Immunofluorescence staining of L22 using a FLAG antibody was performed. **C.-D.** Representative images (100x objective, bar: 40  $\mu\text{m}$ ) of the nuclear (DAPI, blue) and L22 (green) staining upon 48 h (**C**) and 72 h knockdown (**D**). **E.** Quantification of cytoplasmic versus nucleoplasmic intensity of the L22 signal. At least 100 cells were quantified for each condition.

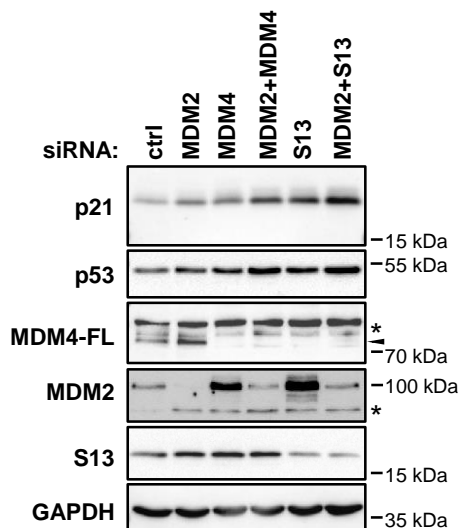
# Figure S5

**A**

RPE 48h siRNA: MDM2, MDM4, S13



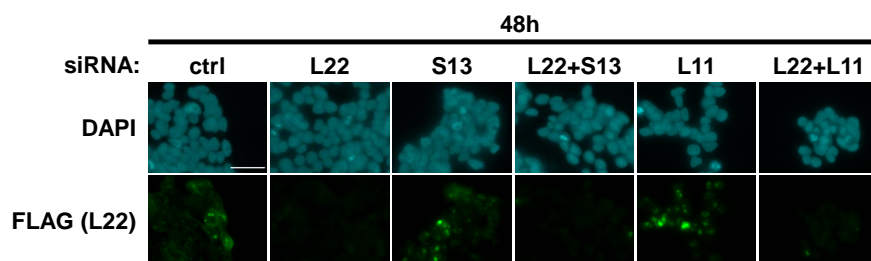
**B**



**C**

HEK293 Flp-In  
L22-FLAG 48h siRNA: L22, S13, L11

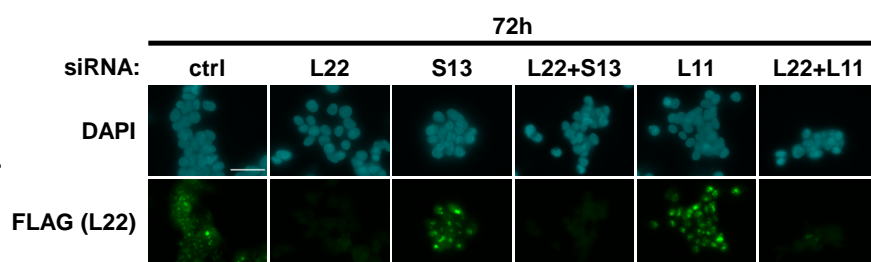
24h tetracycline



**D**

HEK293 Flp-In  
L22-FLAG 72h siRNA: L22, S13, L11

48h tetracycline



**E**

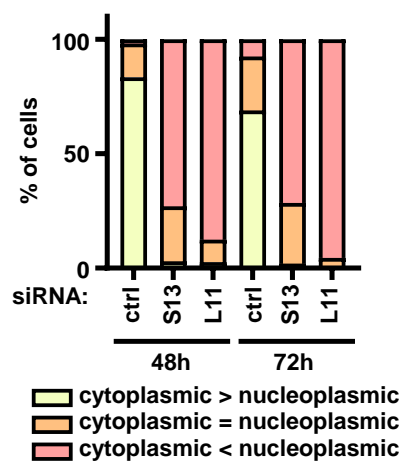


**Figure S6: Conserved L22-binding sequences in *MDM4* intron 6 sustaining p53 activity.**

**A.** Corresponding to [Figure 2B, C](#). Sequence of exon 6 (marked in yellow) and part of intron 6 of the human and murine *MDM4* genes. Sequences in intron 6 predicted to form L22-binding stem loops are marked in green, and the characteristic bases G, C and U (T) are indicated in bold. Nucleotide differences in the murine compared to the human gene are marked in grey. **B.** Corresponding to [Figure 2B, C](#). Genotyping PCR products of RPE Cas9 and RPE *MDM4*  $\Delta$  intron 6 cells were sequenced using a reverse sequencing primer binding at the 3' end of the reverse genotyping primer. The following sequences are marked as also indicated in the figure: 3' end of *MDM4* exon 6 (yellow frames), upstream (us) and downstream (ds) crRNA binding sites (RPE Cas9) respectively parts thereof (RPE *MDM4*  $\Delta$  intron 6) (red frames), protospacer-adjacent motif (PAM) sequences (black frames), sequences predicted to form L22-binding stem loops (green frames). In addition, the binding site of the upstream (forward) genotyping primer respectively its 3' end is marked with a dark blue line. **C.-D.** Corresponding to [Figure 2D-G](#). RPE Cas9 or RPE *MDM4*  $\Delta$  intron 6 cells were transfected with siRNA to deplete L22 and/or S13 for 48 h. **C.** RT-qPCR analyses with normalization to *36B4*. Statistical significance (n = 3): ns, not significant; \*, P $\leq$ 0.05; \*\*, P $\leq$ 0.01; \*\*\*, P $\leq$ 0.001; \*\*\*\*, P $\leq$ 0.0001. **D.** Western blot analysis (n = 2).

# Figure S6

**A**

**MDM4**

**Human**

5' **ATGCTGCTCAGACTCTCGCTCTCGCACAGGATCACAGTATGGATATTCCAAGTCAAGACCAACTG**  
**AAG**GTAAAATCACCACACGGTGACTCTTTTGTGTACAGAGTGGCCCTTCTCTGTACCTATGGA  
TCTTGGACTCCAAGACCTTCCCTGAATGTGGTAAGAATTAATAAGAAAGGTTCTTGGGAGTTC  
ACAGACCAGGGACAGAGTGAACCTTCTCTGTTCTGCCATAACAGAGTTCAGTCTCTGAACCTT  
TCTTTGGGATGTAGCACTTCTGATCTTCAGTCTTCCAGTTGCATTTTTCTTTGGGTTGTGTGAC  
CTGTGTG 3'

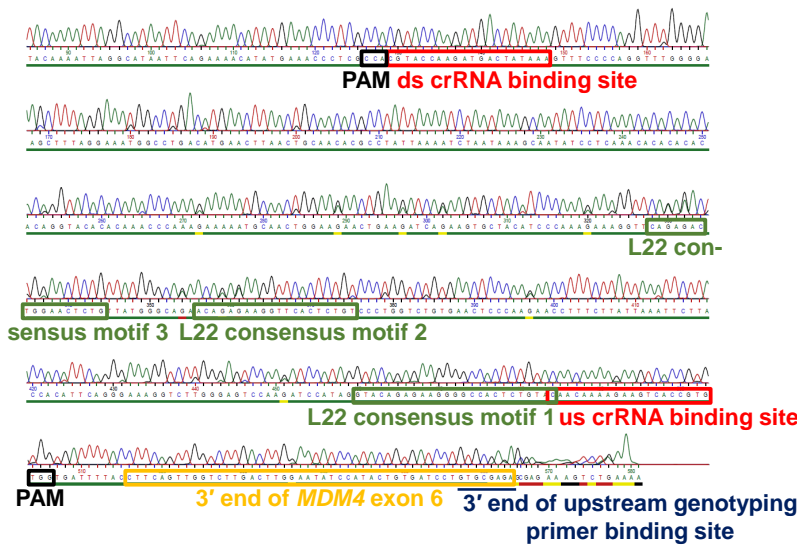
**Mouse**

5' **ATGCTGCTCAGACTCTCGCTCTCGCACAGGATCACAC**TATGGATT**TTCCAAGTCAAGACCAACTG**  
**AAG**GTAAAATCACCACACGGTGACTCTTTTCTGTACAGAGTGGCCCTTCTCTGTACCTGTGG  
ATCTTGGCTCCCAAGCCCTTTCTGTAATGTGGTAAGGATTTAATAAGAAAAGCCCTTGGGAGT  
TCACAGACCAGGGACAGAGTGAACCTTCTCTGTTCTGCCCTTAACAGAGTTCAGTCTCTGAATG  
TCTCTTTGGGATGTAGCACTTCTGATTTCACTCTCCAGTTCTCTCTCTTCTCTCCGCTATT  
TCTGTGCGT 3'

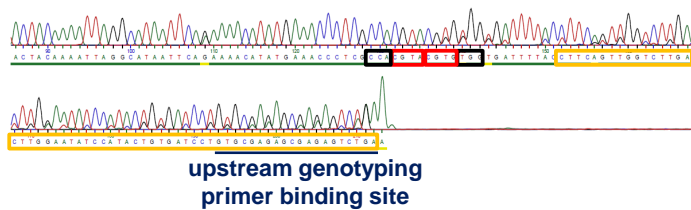
- exon
- L22 motif
- deviations between human and mouse gene

**B**

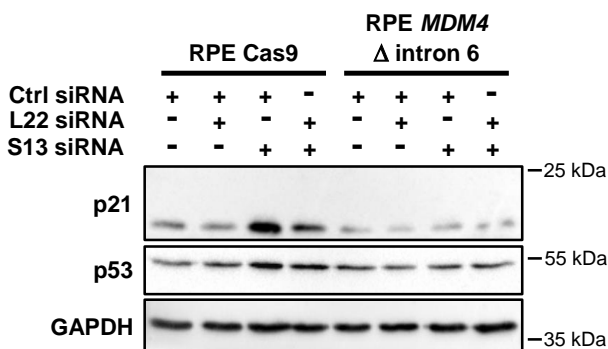
**RPE Cas9**



**RPE MDM4 Δ intron 6**



**D**



**C**

RPE Cas9 or  
RPE MDM4 Δ

intron 6 48h siRNA: L22, S13

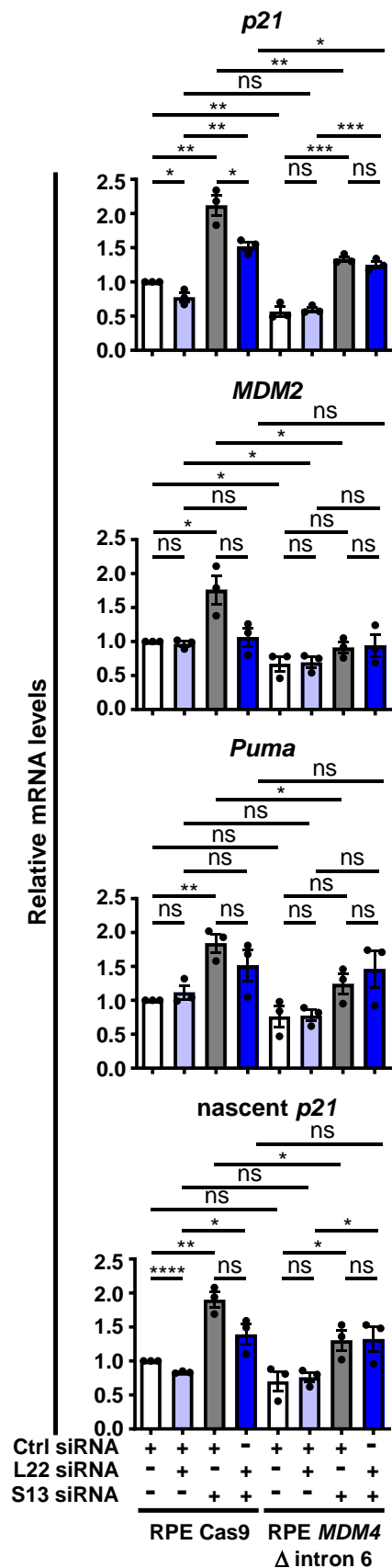
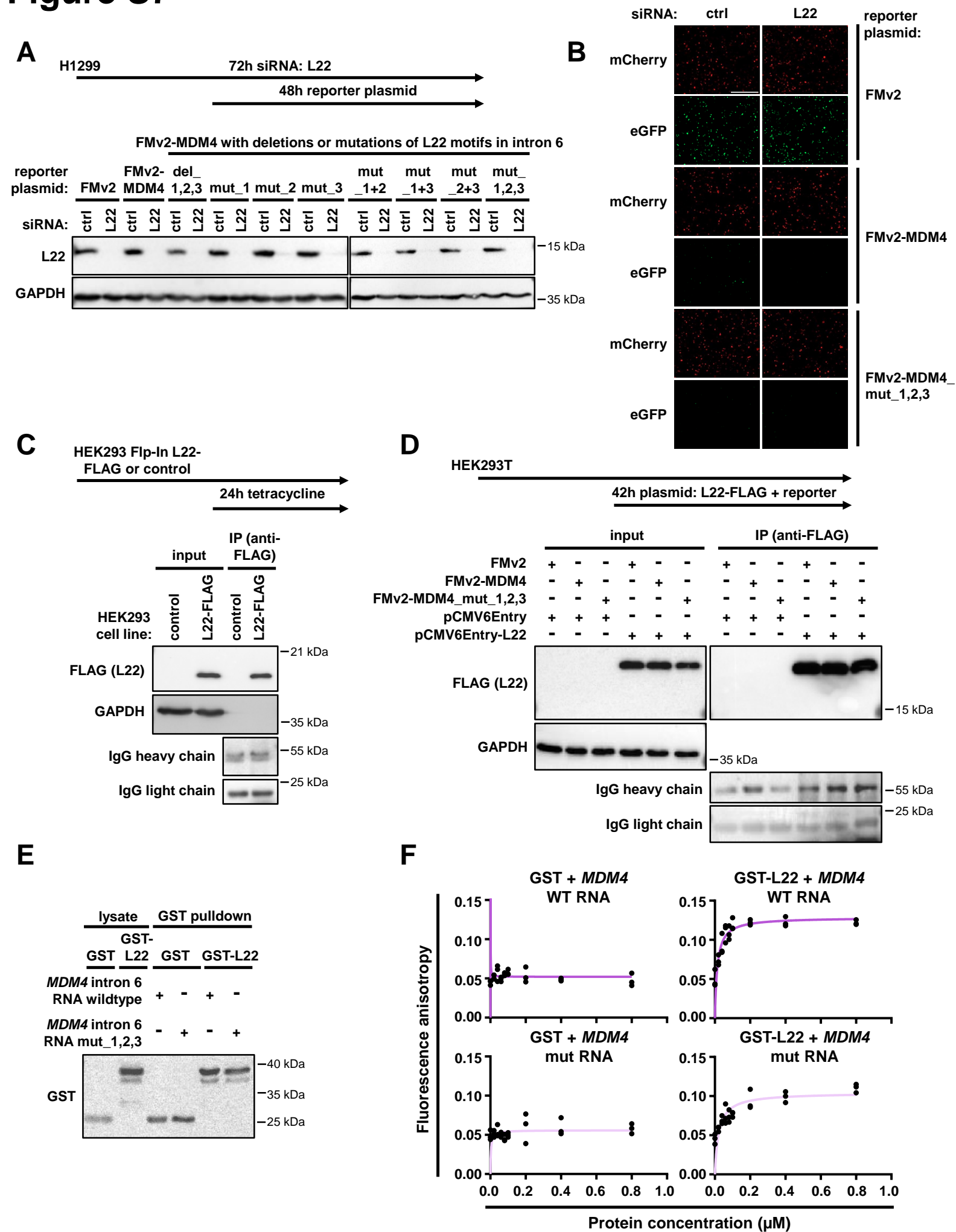


## Figure S7: Association of L22 with RNA corresponding to *MDM4* intron 6.

**A.-B.** Corresponding to [Figure 5A](#), [B](#). Reporter assay. H1299 cells were transfected with siRNA to deplete L22 for 72 h, and with FMv2, FMv2-MDM4 and the different mutated versions of FMv2-MDM4, at 24 hours after the siRNA transfection, followed by incubation for 48 h. **A.** Western blot analysis was performed to confirm L22 depletion, using GAPDH as a loading control (n = 2). **B.** Red fluorescence (mCherry) and green fluorescence (eGFP) were detected. Shown are representative (n = 2) images (5x objective, bar: 800  $\mu$ m) for FMv2, FMv2-MDM4 and FMv2-MDM4\_mut\_1,2,3 reporter plasmids. **C.-F.** RNA-protein binding assays. **C.** Corresponding to [Figure 5C](#). Stably transfected HEK293 Flp-In cells, or parental control cells, were treated with tetracycline (1  $\mu$ g/mL) for 24 h to induce the expression of FLAG-tagged L22, followed by RNA immunoprecipitation (RIP). L22-FLAG expression and precipitation were confirmed by Western blot analysis (n = 2). **D.** Corresponding to [Figure 5D](#). HEK293T cells were transfected with pCMV6Entry or pCMV6Entry-L22 and with either FMv2, FMv2-MDM4 or FMv2-MDM4\_mut\_1,2,3 for 42 h, followed by RIP using FLAG beads to precipitate tagged L22. Overexpression and precipitation of L22 were confirmed by Western blot analysis (n = 2). **E.** Corresponding to [Figure 5E](#). Western blot analysis was performed to confirm the expression and pulldown, using glutathione beads, of GST and GST-L22 incubated with wildtype or mutant *MDM4* transcripts (n = 2). **F.** Corresponding to [Figure 5F](#). Different concentrations of GST or GST-L22 proteins, ranging from 0  $\mu$ M to 0.8  $\mu$ M, were incubated with 20 nM of 3' fluorescein (FAM)-labelled RNA, comprising the wildtype (WT) or mutated (mut) sequence of the first L22 consensus motif in *MDM4* intron 6, and fluorescence anisotropy was measured. Fluorescence anisotropy was plotted against the protein concentrations for the different combinations of GST or GST-L22 with *MDM4* WT (dark purple) or mut (light purple) RNA. Single measurements and fitting curves for three replicates are depicted.

# Figure S7



## Supplementary tables and titles

Tables S1-7, all corresponding to the key resources table (oligonucleotides).

**Table S1: RT-qPCR and reverse transcription primers.** For all: source, Metabion; identifier, N/A.

Primer (DNA oligonucleotide)	Sequence
36B4 forward (V. Manzini)	5'-GATTGGCTACCCAACCTGTTG-3'
36B4 reverse (V. Manzini)	5'-CAGGGGCAGCAGCCACAAA-3'
L22 forward	5'-AGCAAGAGCAAGATCACCGT-3'
L22 reverse	5'-AACTACGCGCAACCAGTCA-3'
L22L1 forward	5'-GGAATGTTGTTACATTGAACGCT-3'
L22L1 reverse	5'-CGAAGCCAATCACGAAGATTGTT-3'
L22L1 mRNA forward	5'-TTTGAGCAATTTCTACGGGAGAAGG-3'
L22L1 mRNA reverse	5'-TGCAACCACTCGAAGCCAA-3'
L22L1 ncRNA forward	5'-TTGGTACCTTCCCTAGTGAATATCT-3'
L22L1 ncRNA reverse	5'-GAAGCCAATCACGAAGATTGTT-3'
MDM2 forward (V. Manzini)	5'-TCAGGATTCAGTTTCAGATCAG-3'
MDM2 reverse (V. Manzini)	5'-CATTTCCAATAGTCAGCTAAGG-3'
MDM4-FL forward (K. Wohlberedt)	5'-CTCAGACTCTCGCTCTCGCA-3'
MDM4-FL reverse (K. Wohlberedt)	5'-CTCAAATCCAAGGTCCAGCCT-3'
MDM4-S forward	5'-CTACTGGGACGTCAGAGCTTC-3'
MDM4-S reverse	5'-CCTCTGCACTTTGCTGTAGTA-3'
Nascent p21 forward (K. Henningsen)	5'-AGACCAGCATGACAGGTGCG-3'
Nascent p21 reverse (K. Henningsen)	5'-GCCTGGCATAATGAACATTCCCA-3'
p21 forward (V. Manzini)	5'-TAGGCGGTTGAATGAGAGG-3'
p21 reverse (V. Manzini)	5'-AAGTGGGGAGGAGGAAGTAG-3'
p53 forward (V. Manzini)	5'-ATGGAGGAGCCGCAGTCAGATC-3'
p53 reverse (V. Manzini)	5'-GGGAGCAGCCTCTGGCATTCTG-3'
Puma forward (V. Manzini)	5'-GACGACCTCAACGCACAGTA-3'
Puma reverse (V. Manzini)	5'-CTAATTGGGCTCCATCTCG-3'
L11 forward	5'-GATCCTTTGGCATCCGGAGAA-3'
L11 reverse	5'-CAGGCCGTAGATACCAATGCT-3'
L5 forward	5'-CAGCGTATGCACACGAACCTG-3'
L5 reverse	5'-AACCTATTGAGAAGCCTGCGG-3'
S13 forward	5'-AGGGACTTGCTCCTGATCTTCC-3'
S13 reverse	5'-ACCAGGGCAGAGGCTGTAGAT-3'
UBAP2L-201 forward	5'-CAGCAGCCGCATTCTCAGAT-3'
UBAP2L-201 reverse	5'-CCAAGCTGGTCATCGACGAAA-3'
UBAP2L-207 forward	5'-TGCCTTCAGCCCTAGGAAGT-3'
UBAP2L-207 reverse	5'-AGCTGTAGCTGTTGTAGGCAG-3'
ZMAT3 forward	5'-ATCCTCAGAGCTGGGTCAAC-3'
ZMAT3 reverse	5'-TGGCCACTTGGAGTAACACA-3'
Oligo-dT	5'-TTTTTTTTTTTTTTTTTTTTTTTTTV-3' with wobble N 3' modification
Random nonamer	5'-NNNNNNNNN-3'

**Table S2: Genotyping and sequencing primers.** For all: source, Metabion; identifier, N/A.

Primer (DNA oligonucleotide)	Sequence
MDM4_sli6all_1 forward	5'-TCAGACTCTCGCTCTCGCAC-3'
MDM4_sli6all_1 reverse	5'-AAGGCAACACCTCTCCTCAAC-3'
MDM4_sli6all_2 forward	5'-TCTCGCACAGGATCACAGTATG-3'
MDM4_sli6all_2 reverse	5'-CCTCAACCCACTGTGAGCAAA-3'

**Table S3: Primers for semi-quantitative detection of *MDM4* and *L22L1* variants.** For all: source, Metabion; identifier, N/A.

Primer (DNA oligonucleotide)	Sequence
L22L1 common forward	5'-TGGACCTTACTCATCCAGTAGA-3'
L22L1 common reverse	5'-GCAACCACTCGAAGCCAATC-3'
MDM4 common forward	5'-TGTCACCTTTAGCCACTGCTACT-3'
MDM4 common reverse	5'-AGTGGAACTTTCCTCTGCACTT-3'
MDM4_exon3+10_cm_3 forward	5'-CAGGTGCGCAAGGTGAAATG-3'
MDM4_exon3+10_cm_3 reverse	5'-AGGTAACCTCTACATCGGTATCA-3'

**Table S4: Primers for RNA-protein binding experiments.** For all: source, Metabion; identifier, N/A.

Primer (DNA oligonucleotide)	Sequence
FMv2 3' eGFP forward	5'-ACTCGCAGACCATTACCAGC-3'
FMv2 3' eGFP reverse	5'-CTTTGCTCAGCGCAGATTGG-3'
MDM4 exon 9/intron 9 forward	5'-TCAGAGCAGTTAGGTGTTGGAA-3'
MDM4 exon 9/intron 9 reverse	5'-GGGATTATGTGAGCAATCTGTTGT-3'
MDM4 intron 6 3' of L22 motifs forward	5'-TGATCTTCAGTTCTTCCAGTTGC-3'
MDM4 intron 6 3' of L22 motifs reverse	5'-TGAACCTTAACTGCAACACGCC-3'
MDM4_in vitro PCR_22 nt_mut reverse	5'-GGTTCAGACTCTGGAAGTCTGT-3'
MDM4_in vitro PCR_22 nt_WT reverse	5'-GGTTCAGAGACTGGAAGTCTGT-3'
MDM4_in vitro PCR_42 nt_mut forward	5'- TAATACGACTCACTATAGGGTTTTGTTGTACA GACTGGCCCC-3'
MDM4_in vitro PCR_42 nt_WT forward	5'- TAATACGACTCACTATAGGGTTTTGTTGTACA GAGTGGCCCC-3'
MDM4_in vitro qPCR_1 forward	5'-AAGACCTTTCCTGAATGTGGT-3'
MDM4_in vitro qPCR_1 reverse	5'-TCTGTCCCTGGTCTGTGAACTC-3'

**Table S5: Primers for reporter plasmid mutagenesis.** For all: source, Metabion; identifier, N/A.

Primer (DNA oligonucleotide)	Sequence
FMv2-MDM4_A1 (A forward)	5'-CATAGGTACAGACTAGGGGCCAGTCTG TACAACAAAAGAAGTCACC-3'
FMv2-MDM4_A2 (A reverse)	5'-GGTGACTTCTTTTGTGTACAGACTGGC CCCTAGTCTGTACCTATG-3'
FMv2-MDM4_B1 (B forward)	5'-GGCAGAACAGACTAGGTTCACTCTGTC CCTGGTCTGTGAAC-3'
FMv2-MDM4_B2 (B reverse)	5'-GTTACAGACCAGGGACAGACTGAACC TAGTCTGTTCTGCC-3'

FMv2-MDM4_C1 (C forward)	5'-AAGAAAGGTTTCAGACTCTGGAAGTCTGT TATGGGCAGAACAGAGAAG-3'
FMv2-MDM4_C2 (C reverse)	5'-CTTCTCTGTTCTGCCATAACAGACTTC CAGAGTCTGAACCTTTCTT-3'
FMv2-MDM4_KO1 forward	5'-GGTAAAATCACCACACACGTGGCGAGGG TTGG-3'
FMv2-MDM4_KO1 reverse	5'-CCAACCCTCGCCACGTGTGTGGTGATTT TACC-3'

**Table S6: Primers for HEK293 Flp-In L22-FLAG cell line generation.** For all: source, N/A; identifier, N/A.

Primer (DNA oligonucleotide)	Sequence
L22_fw_Kozak_BamHI	5'-ATATATGGATCCGCCACCATGGCTCCTGTG AAAAAGCTTGTGG-3'
L22_rv_NheI_nostop	5'-ATATATGCTAGCATCCTCGTCTTCCTCCTCT TCTTCG-3'

**Table S7: RNA oligonucleotides.**

RNA oligonucleotide	Source	Identifier
Alt-R CRISPR-Cas9 tracrRNA	Integrated DNA Technologies	Order# 3319514
crRNA MDM4_sli6 all_1 TTTATAGTCATCTTGGTACG	Integrated DNA Technologies	Order# 3657380
crRNA Mdm4i61 CAACAAAAGAAGTCACCGTG	Integrated DNA Technologies	Order# 3319514
MDM4_I6_L22BM_MUT	Integrated DNA Technologies	Order# 238303092
MDM4_I6_L22BM_WT	Integrated DNA Technologies	Order# 238303091
siRNA ctrl(-1) (ssc1)	Thermo Fisher Scientific	Cat# 4390844
siRNA ctrl(-2) (targeting luciferase)	Thermo Fisher Scientific	Cat# s237070, 4399665
siRNA ctrl(-3) (targeting luciferase)	Thermo Fisher Scientific	Cat# s237071, 4399665
siRNA L22(-1)	Thermo Fisher Scientific	Cat# s12190
siRNA L22-2	Thermo Fisher Scientific	Cat# s12191
siRNA L22L1	Thermo Fisher Scientific	Cat# s47290
siRNA MDM2	Thermo Fisher Scientific	Cat# cs
siRNA MDM4	Thermo Fisher Scientific	Cat# s8631
siRNA L11	Thermo Fisher Scientific	Cat# s12168
siRNA L5	Thermo Fisher Scientific	Cat# s12151
siRNA S13(-1)	Thermo Fisher Scientific	Cat# s12304
siRNA S13(-2)	Thermo Fisher Scientific	Cat# s12305
siRNA ZMAT3	Thermo Fisher Scientific	Cat# s34677